Journal of Theoretical and Applied Information Technology
20th February 2013. Vol. 48 No.2

ISSN: 1992-8645 www.jatit.org E-ISSN: 1817-3195

MODELING AND TRANSIENT DYNAMICS ANALYSIS TO A NEW TYPE OF ENGINE PISTON

[1]HONGYUAN ZHANG, [2]XINGGUO MA, [1]SHUANGLIANG GE

[1]School of Automobile and Traffic, Shenyang Ligong University, Shenyang 110159, Liaoning, China

[2]School of Mechanical Engineering, Shenyang Ligong University, Shenyang 110159, Liaoning, China

ABSTRACT

This paper introduces of a new structure which applies the round slider of the crank instead of the connecting rod. Based on the motion equation of the transient dynamics as the basis, this paper carries out transient kinetic analysis to the piston with the complete method, thus obtaining the displacement nephogram and the stress nephogram of the piston and analyzing the response of the displacement to the time and the stress to the time for the piston, thus obtaining the position of the maximum displacement and stress of the piston and the dangerous moment. Results show that, with the greater safety factor of the piston, it is possible to further improve the performance of the engine with the structure improvement.
Keywords: *Transient Dynamics, Finite Element Method, Engine, Piston*

1. INTRODUCTION

The crank round slider engine consists of two pistons, two eccentric round sliders, a dynamic balance slider and a single crank, a connecting rod in a crank connecting rod engine is replaced by the eccentric round slider, and the dynamic slider substitutes for crank balance to play the role of balance. Because the crank and the connecting rod of the structural engine have equal lengths and the piston of particular structure is adopted, the stroke of the piston is 4 times that of the crank. An engine of the same volume has a stroke much bigger than a traditional engine, the piston does work on both sides and a crankcase is eliminated, so that the structure is reduced obviously with the advantages of simple structure, small volume, and stable operation and so on.

The existing work to finite element analysis of piston as follows, Evangelos G. Giakoumis[1] have studied lubricating oil effects on the transient performance of a turbocharged diesel engine. Ali Abdul-Aziz, Michael T. Tong[2] using finite-element, transient heat transfer analyses were performed for the first-stage blades of the space shuttle main engine high-pressure fuel turbo pump. Joseph Padovan, Mike Adams, Demeter Fertis, Ibrahim Zeid, Paul Lam[3] extends the finite element scheme to handle the highly nonlinear interfacial fields generated in the fluid filled annulli of squeeze film and journal bearings so as to model the transient response of rotor-bearingstator systems.S. Boedo, J.F. Booker[4] analysis transient dynamics of engine bearing systems. J. Padovan, O. Paramodilok[5] described a finite element methodology which can handle the transient response of moving structures which are themselves subject to time dependent traveling load fields. F.K. Choy, J. Padovan[6] investigates the problem of the non-linear dynamics of rotor/casing rub interactions in rotating equipment.

The piston is one of the most important parts of the engine and the mechanical performance directly determines the performance of the engine. Based on the transient dynamics equation, this paper establishes the finite element model of piston by using the finite element software, divides a period of pressure curve into twenty load steps, carries out transient dynamics analysis to the piston by using the complete method in order to obtain the piston displacement, stress nephogram and the response curve, and provides the basis for the optimization design of the piston.

2. PISTON MODEL

The piston of the engine is a special double-headed piston. Different from the traditional piston, crank circular slide block replaces the crank connecting rod mechanism because the structure of the piston is symmetrical. In order to calculate conveniently, 1/4 model is introduced, as shown in Figure 1.

Journal of Theoretical and Applied Information Technology
20th February 2013. Vol. 48 No.2

ISSN: 1992-8645 www.jatit.org E-ISSN: 1817-3195

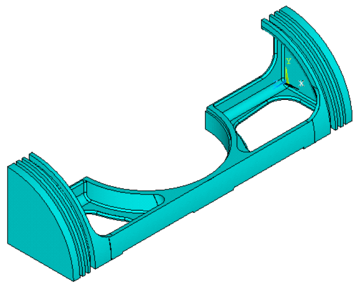

Figure 1: Three-Dimensional Model Of The Piston

The piston adopts cast iron as the material and its finite element grid partition uses the hexahedral elements. The grid division employs the intelligent grid partition and it chooses 8 nods and Solid 45 unit. The piston division produces 11671 nods and 38297 units. The material properties of the piston are shown in Table 1.

Table 1: The Material Properties Of The Piston

properties	parameters
material	qt800
elastic modulus	150 GPa
poisson ratio	0.3
density	7800 g/mm^3

3. TRANSIENT DYNAMICS ANALYSIS

3.1 Basic Equations for Transient Dynamics Analysis

The transient dynamics analysis is a method of dynamics response to determine the structure of load which changes with the time. It can analyze the displacement, strain and stress changes with the time under the state of static load, transient load and harmonic load and the combination function. Load and time correlation makes the force of inertia and damping effect obviously. If the inertia force and the damping effect are not obvious, static analysis can replace the transient analysis. The basic motion equations of transient dynamics analysis is

$$[M^e]\{\ddot{a}(t)^e\}+[C^e]\{\dot{a}(t)^e\}+[K^e]\{a(t)\}^e=\{Q(t)^e\} \quad (1)$$

Where:

$[M^e]$ = Mass matrix

$[C^e]$ = Damping matrix

$[K^e]$ = Stiffness matrix

$\{\ddot{a}(t)\}$ = Accelerator vector of the node

$\{\dot{a}(t)\}$ = Velocity vector of the node

$\{a(t)\}$ = Displacement vector of the node

In the any given time of t, these equations can be considered as a series of static equilibrium equations which take into consideration the inertia force ($[M^e]\{\ddot{a}(t)\}$) and the damping force ($[C^e]\{\dot{a}(t)\}$). The ANSYS program solves these equations with the Newmark time integration method at discrete time points. The time increment between the connected time points are called integration time step.

3.2 Applying Constraint

Because of piston symmetry, apply symmetry constraint to the model of the piston, to restrict the displacement in directions of X-axial and Y-axial and the model with applied constraint is as shown in Figure 2.

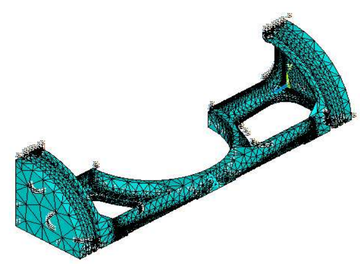

Figure 2: Models With Applied Constraint

3.3 Applying Load

The loads applied to the piston in the cycle before are divided into several steps of loads; apply the corresponding loads of each moment to the piston and the whole process is divided into 20 steps of load application and the applied time and the corresponding loads are as shown in Table 2.

Table 2 : Table Of The Applied Values

	Time (SEC)	Force of the circular slider to the piston (P_a/m^2)	Gas pressure to the left side of the piston (P_a/m^2)	Gas pressure to the right side of the piston (P_a/m^2)
1	1.333333e-4	1.853158e4	2.83337e3	2.53199e4
2	4.000000e-4	1.688329	2.60951e3	2.55138e4
3	6.666667e-4	4.534774e3	2.45537e3	2.49961e4
4	8.000000e-4	1.253394e4	2.31265e3	2.41124e4

ISSN: 1992-8645 www.jatit.org E-ISSN: 1817-3195

5	1.333333e-3	4.717193e2	1.77881e3	1.94750e4
6	2.933333e-3	1.223983e4	1.11882e3	1.10448e4
7	4.800000e-3	1.938386e2	6.89001e2	5.41200e3
8	5.733333e-3	9.754406e2	3.92726e3	1.07747e4
9	7.600000e-3	2.194009e3	3.31041e3	2.28509e4
10	1.013333e-2	2.526969e4	2.85832e3	3.95927e2
11	1.040000e-2	2.555230e4	2.60168e3	3.330528e3
12	1.266667e-2	1.199736e4	1.18908e3	2.17118e4
13	1.426667e-2	6.698565e3	6.90309e2	1.33250e4
14	1.453333e-2	5.991361e3	6.52344e2	1.99354e4
15	1.480000e-2	5.406410e3	6.844595e2	2.50763e4
16	1.653333e-2	3.517283e3	1.421925e3	2.90171e2
17	1.826667e-2	3.209960e3	2.761895e3	1.15563e4
18	1.933333e-2	3.049950e3	5.471146e3	7.53557e3
19	1.986667e-2	2.980806e3	2.44029e4	2.08291e4
20	2.000000e-2	2.975109e3	2.50000e4	2.00061e4

4. RESULT ANALYSIS

4.1 Displacement and Stress

We define that the analysis type of the definite elements of the piston is the transient kinetic analysis and select the complete method to carry out analysis. The transient kinetic analysis of the piston is divided into 20 load steps. Select four load steps which can make different to the piston analysis to carry out analysis to the deflection, as shown from Figure 3 to Figure 6. During the first load step, the piston is in the neutral position and begins to get prepared for moving. Figure 3 is the displacement nephogram in the direction of the X-axial in the first load step, with the maximum displacement, the minimum displacement, the load step and the time marked on the top left corner and the color band indicating the size of the displacement at the bottom. According to color distribution of the piston, we can clearly see the position of the maximum displacement at the piston. Figure 4 is the displacement nephogram of the fifth load step, when the piston is the suction stroke, the piston moves from the left to the right and the maximum displacement occurs at the end of the piston. Figure 5 is the displacement nephogram of the ninth load step when the piston begins to move to the left and gets ready for the next stroke. Figure 6 is the displacement nephogram of the thirteenth load step.

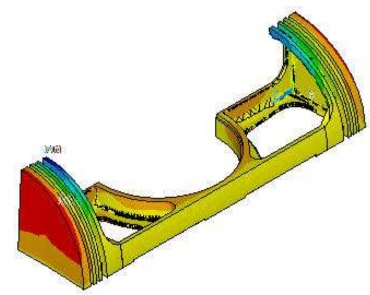

Figure 3: The Displacement Nephogram In The First Load Step

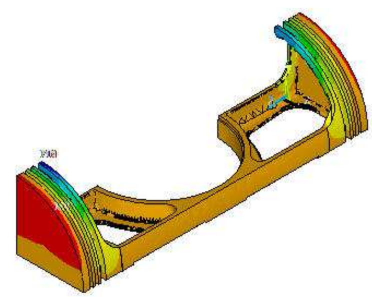

Figure 4: The Displacement Nephogram Of The Fifth Load Step Of The Piston

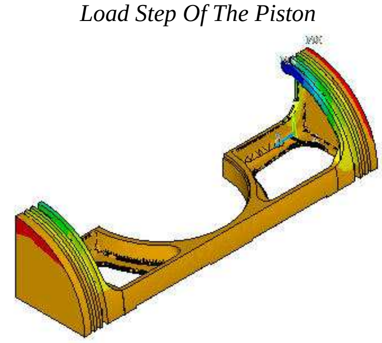

Figure 5: The Displacement Nephogram Of The Nineteenth Load Step Of The Piston

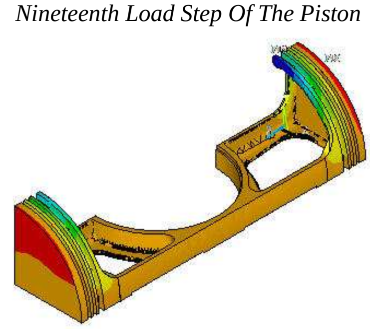

Figure 6: The Displacement Nephogram Of The Thirteenth Load Step Of The Piston

Journal of Theoretical and Applied Information Technology
20th February 2013. Vol. 48 No.2

ISSN: 1992-8645 www.jatit.org E-ISSN: 1817-3195

Figure 7 to Figure 12 are stress nephogram of the piston, when we can see the entire and partial stress of the piston directly. Express the deformed image of the piston when completing a cycle, select several typical load step analysis and take the stress nephogram of the piston in the direction of the Z-axial as an example to illustrate the stress condition of the piston. Figure a is the stress nephogram of the first load step.

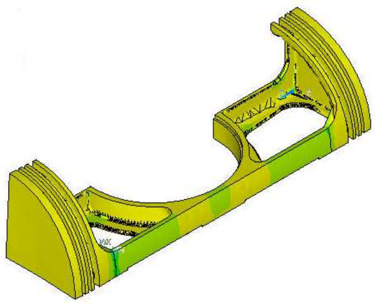

Figure 7: Stress Nephogram Of The First Load Step Of The Piston

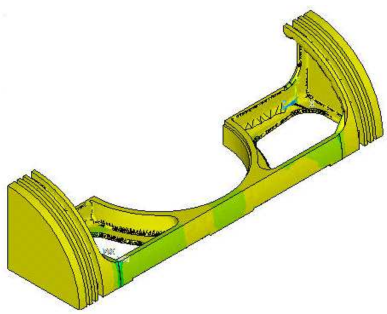

Figure 8: Stress Nephogram Of The Fifth Load Step Of The Piston

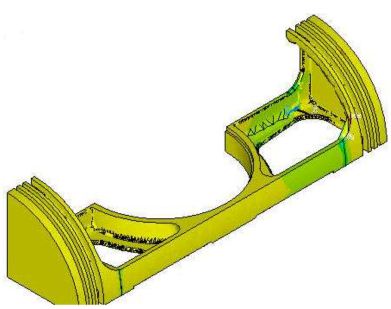

Figure 9: Stress Nephogram Of The Nineteenth Load Step Of The Piston

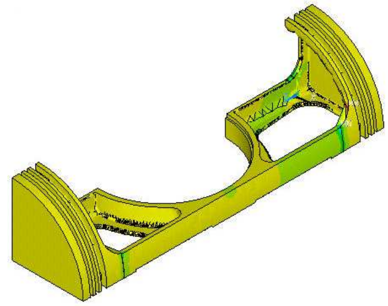

Figure 10: Stress Nephogram Of The Thirteenth Load Step Of The Piston

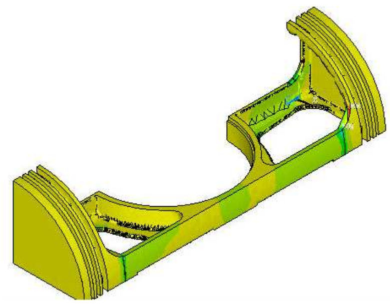

Figure 11: Stress Nephogram Of The Seventeenth Load Step Of The Piston

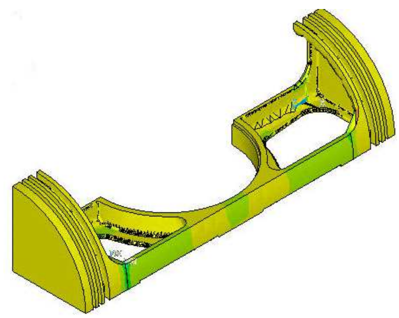

Figure 12: Stress Nephogram Of The Nineteenth Load Step Of The Piston

From Figure 7 to Figure 12, we can see that the stress concentration phenomenon occurs at the reinforcing rib where the piston crown is connected to the aperture of the circular slider, which we should pay attention to when designing so as to reduce stress concentration.

4.2 Response of the Displacement and the Stress to Time

Divide the motion cycle of acting once into 20 load steps, i.e. each load step corresponds to a time and a displacement of the piston, as shown in Figure 5. E.g., when we observing the piston at the moment of 5.733333e-3 with the decoder, the maximum node of the displacement at the Y-axial

ISSN: 1992-8645 www.jatit.org E-ISSN: 1817-3195

is 243, this is the condition of the fifth load step and then we can observe these results with the processor POST26 after time history. POST26 is used to observe the result of the fixed point in the model which is expressed as the time function. Figure 13 shows the response curve of the displacement of node 243 based on the time.

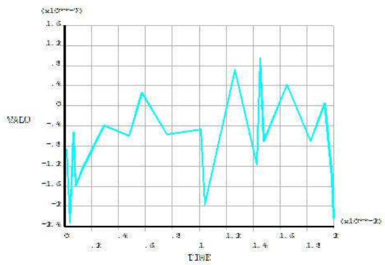

Figure 13: The Displacement- Time Response Curve Of Node 243

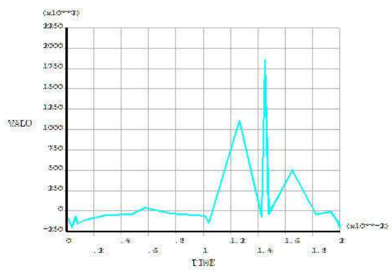

Figure 14: The Stress-Time Response Curve Of Node 7833

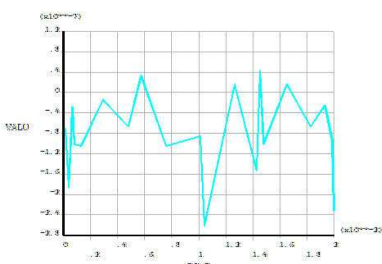

Figure 15: The Displacement- Time Response Curve Of Node 99

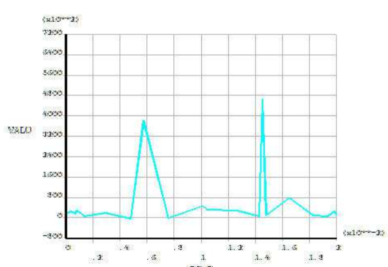

Figure 16: The Stress- Time Response Curve Of Node 7872

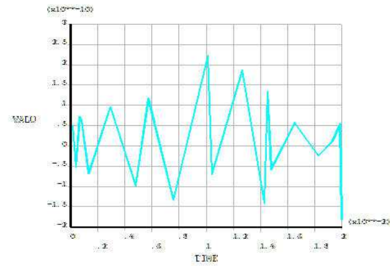

Figure 17: The Displacement- Time Response Curve Of Node 99

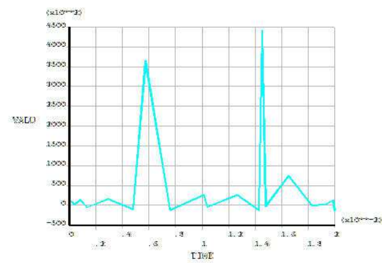

Figure 18: The Stress-Time Response Curve Of Node 7872

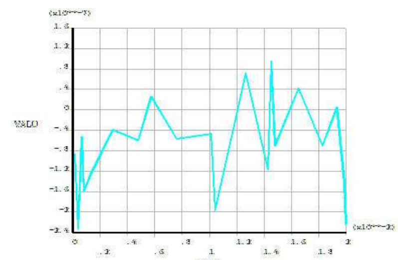

Figure 19: The Displacement- Time Response Curve Of Node 243

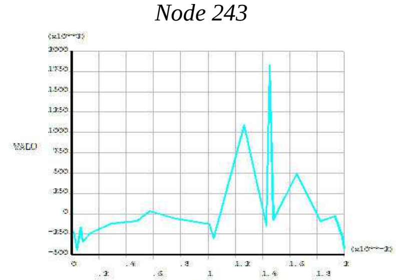

Figure 20: The Stress-Time Response Curve Of Node 7833

Figure 14 is the stress change curve with the time in the first strength theory. When we find out the fifth load step in the computation result menu, the node with the maximum stress is at 7833 and then checks that the corresponding unit is 18254. At the tenth load step, i.e. at the moment of 1.013333e-2, the node with the maximum displacement variation is at 99 and the displacement-time changing diagram of this the node is as shown in Figure 15. Figure 16 is the stress-time changing curve figure in the first strength theory; when we find out the tenth load step in the computation result menu, the

ISSN: 1992-8645 www.jatit.org E-ISSN: 1817-3195

node with the maximum stress is at 7872 and then checks that the corresponding unit is 18254. At the fifteenth load step, i.e. at the moment of 1.480000e-2, the node with the maximum displacement variation is at 99 and the displacement-time changing diagram of this the node is as shown in Figure 17. Figure 18 is the stress-time changing curve figure in the first strength theory; when we find out the fifteenth load step in the computation result menu, the node with the maximum stress is at 7872 and then check that the corresponding unit is 19300. At the nineteenth load step, i.e. at the moment of 1.986667e-2, the node with the maximum displacement variation is at 243 and the displacement-time changing diagram of this the node is as shown in Figure 19. Figure 20 is the stress-time changing curve figure in the first strength theory; when we find out the nineteenth load step in the computation result menu, the node with the maximum stress is at 7833 and then check that the corresponding unit is 18256.

In overall consideration of the stress-time changing curves as stated above, it is easy to figure out from the figures that the corresponding moment of the maximum stress calculated with the first strength theory is approximately at 1.5e-2 second; because the dangerous moments are almost the same in several figures, the maximum stress is not only the dangerous moment of a certain node of the piston for the use of a certain unit, but also the entire dangerous moment for the piston. From Table 2 we can get that the maximum stress value is 2.5615MPa when the dangerous moment is at Second 1.480000e-2 and that the piston is at the working condition of explosion. From the working manual, we can get that at the dangerous moment the maximum stress value meets the stress requirements for cast iron. So, the selection of the piston should meet the requirements for the working condition.

5. CONCLUSION

With the transient dynamics analysis to a new type of engine piston, we have obtained the displacement and stress nephogram of the piston and with the analysis to the displacement and the stress response to time; we have also obtained the maximum position and the dangerous moment for the stress and the displacement of the piston. From the result, we get that the safety factor of the piston is relatively large. We can reduce the piston quality with structure optimization, thus further decreasing the reciprocating inertia force of the piston and improving the engine performance.

REFERENCES:

[1] Evangelos G. Giakoumis, "Lubricating oil effects on the transient performance of a turbocharged diesel engine", *Energy*, Vol. 35, No. 2, 2010, pp. 864-873.

[2] Ali Abdul-Aziz, Michael T. Tong, "Thermal finite-element analysis of space shuttle main engine turbine blade", *Finite Elements in Analysis and Design*, Vol. 5, No. 4, 1989, pp. 337-348.

[3] Joseph Padovan, Mike Adams, Demeter Fertis, Ibrahim Zeid, Paul Lam, "Nonlinear transient finite element analysis of rotor-bearing-stator systems", *Computers & Structures*, Vol. 18, No. 4, 1984, pp. 629-639.

[4] S. Boedo, J.F. Booker, "Transient dynamics of engine bearing systems", *Tribology Series*, Vol. 14, 1989, pp. 323-332.

[5] J. Padovan, O. Paramodilok, "Generalized solution of time dependent traveling load problem via moving finite element scheme", *Journal of Sound and Vibration*, Vol. 91 , No. 2, 1983, pp. 195-209.

[6] F.K. Choy, J. Padovan, "Non-linear transient analysis of rotor-casing rub events", *Journal of Sound and Vibration*, Vol. 113, No. 3, 1987, pp. 529-545.

[7] G.F. Dargush, P.K. Banerjee, "Boundary element methods for three-dimensional thermoplasticity", *International Journal of Solids and Structures*, Vol. 28, No. 5, 1991, pp. 549-565.

[8] Richard W.H. Wu, Emmett A, "Witmer.The dynamic responses of cylindrical shells including geometric and material nonlinearities", *International Journal of Solids and Structures*, Vol. 10, No. 2, 1974, pp. 243-260.

[9] S. Roques, M. Legrand, P. Cartraud, C. Stoisser, C. Pierre, "Modeling of a rotor speed transient response with radial rubbing", *Journal of Sound and Vibration*, Vol. 329, No. 5, 2010, pp. 527-546.

[10] C.Soize, "Transient responses of dynamical systems with random uncertainties", *Probabilistic Engineering Mechanics*, Vol. 16, No. 4, 2001, pp. 363-372.

[11] Richard H. Gallagher, "Finite element analysis in brittle material design", *Journal of the Franklin Institute*, Vol. 290, No. 6, 1970, pp. 523-537.